Data-Hiding Capacities of Non-Redundant Complex Wavelets

Lahouari Ghouti

School of Computer Science, Queen's University of Belfast.
Belfast BT7 1NN, United Kingdom.
Email: L.Ghouti@qub.ac.uk

Keywords: Digital watermarking, data hiding capacity, non-redundant complex wavelets, game-theoretic bounds, information-theoretic bounds.

Abstract

In this paper, we apply an information-theoretic model, developed for digital image watermarking, to derive the data-hiding capacities of image sources in the mapping-domain of non-redundant complex wavelet transforms (NCWTs). Results, based on the same model, have been recently reported for balanced multiwavelet (BMW) transforms. In this model, the underlying statistical model defines the hiding capacity in terms of the distortion constraints imposed on the watermark embedder and the attacker, and the information available to the watermark embedder, to the attacker, and to the watermark decoder. The motivations behind the use of NCWTs is the directionality and phase information provided by such representations.

1 Introduction

With the rapid growth and widespread use of network distributions of digital media content, there is an urgent need for protecting the copyright of digital content against piracy and malicious manipulation. Recently, watermarking systems have been proposed as a possible and efficient answer to these concerns. Digital watermarking refers to embedding an auxiliary signal (called watermark) within a host signal such as text, audio, image, or video. This embedding should be nearly imperceptible and robust against possible (intentional and accidental) manipulations of the watermarked data such that one can reliably recover the watermark even if the host and watermark signals undergo a variety of tampering and attacks as long as these manipulations do not unacceptably degrade the host signal. Information hiding methods have numerous applications such as covert communications, authentication, proof of ownership, customer tracing, and data embedding. Copyright protection represents the focus of most of these applications. Over the last decade, watermarking research has focused mainly on developing news paradigms for watermark embedding and detection. However, in the last few years there was less obsession with this goal; rather, information-theoretic watermarking research began to emerge [1]. In particular, a theory has recently been developed to establish the fundamental limits of the watermarking (data-hiding) problem. Around the same time, Cox et al. [2] have also recognized that one may view watermarking as communications with side information known at the encoder. This is reminiscent of the communications problem with a fixed noisy channel, and side information at the encoder [2]. Interestingly enough, Chen and Wornell [2] were the first to establish the analogy between watermarking and communications with side information problems. The goal of this paper is to derive the watermarking (data-hiding) capacity estimates for mapping-based NCWT transforms [3] using various statistical models for the host image. Section II outlines the mathematical properties of redundant and non-redundant CWT transforms and the motivation behind the use of non-redundant CWTs in digital watermarking applications. Section III describes the basic statistical model for the image watermarking problem. Then, we will derive the data-hiding capacity for NCWTs using various channel models.

2 Redundant and Non-Redundant CWTs

Unlike the discrete wavelet transform (DWT), complex wavelet transforms (CWTs) offer three significant advantages: 1) directionality, 2) explicit phase information, and 3) shift-invariance [3]. The shift-invariance property in the DWT, inherent to the use of the downsamplers [3], makes that the DWT coefficients fail to discriminate between the shifts of the processed content. The DWT coefficients are able to reveal only specific feature orientations present in the spatial domain. Furthermore, the DWT has poor directional selectivity for diagonal features, which is evident from the impulse responses of the filters of individual subbands. There is only one filter for diagonal features. In the complex transforms, the real and imaginary parts form an approximate Hilbert-transform pair [3]. Furthermore, the properties, provided by these transforms, enable efficient statistical modeling for the subbands' coefficients. Such modeling has an important *geometric* interpretation that has crucial importance in image coding and watermarking applications [3]. It should be noted that the undecimated DWT transform has been proposed as a solution to overcome the shift-invariance limitation at the expense of an increased computational complexity while suffering the same poor selectivity for the diagonal features. On the other hand CWT-based solutions are more computationally efficient and have only a controllable redundancy; yet they provide approximate shift invariance and good directional selectivity. In what follows, we will give a brief overview of redundant and non-redundant CWTs.

2.1 Redundant Complex Wavelet Transforms

Abry [3] propose a novel transform that consists of a pair of real wavelets such that they form a Hilbert relation (i.e., one is the Hilbert transform of the other). Then, the CWT consists of the pair of DWT trees that implement the DWTs associated with the wavelet pair. Subband coefficients emanating from both pairs represent the real and imaginary parts of the complex subband coefficients, respectively. Also, Abry's solution can be implemented using a single DWT tree based on a quasi-analytic wavelet [3]. However, it should be noted that quasi-analytic DWT is not invertible, therefore, it cannot be used in image applications requiring processing. Kingsbury [3], to overcome this disadvantage, propose the dual-tree wavelet transform (DTWT), which is a quadrature pair of DWT trees similar to those proposed in Abrys solution. Though the DTWT transform is invertible and achieves approximate shiftability, the filter design is quite complicated. Fig. 1 shows the directionality property of the DTWT where opposite diagonal directions can be efficiently distinguished due to the presence of two different filters to represent the diagonal features. It should be noted that the redundancy in DTWT is $4:1$. At each decomposition level, there are six detail subbands, instead of three subbands as in the DWT case. Actually, the inherent redundancy of the DTWT puts severe restrictions on the design of any watermarking scheme since there is no guarantee that the DTWT modified coefficients will lead to a valid image representation in the spatial domain.

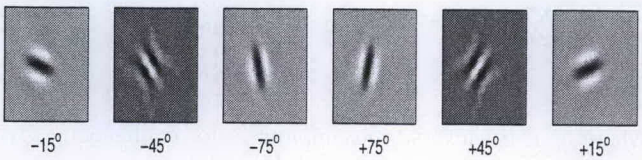

Figure 1: 2D Filter impulse responses for the DTWT.

2.2 Non-Redundant Complex Wavelet Transforms

In order to have a sparse representation for CWTs, Felix et al. [3] propose a mapping-based CWT. The proposed CWT is characterized by a decoupled implementation that has two major merits. First, the controllable redundancy of the mapping stage offers a balance between degree of shift sensitivity and transform redundancy. The second merit is the flexibility to use any DWT kernels in the transform implementation unlike the DTWT which is based on a specific set of filters [3]. Furthermore, the first merit enables the design of a directional and non-redundant CWT that has potential benefits for image watermarking systems. It worth noting that such an implementation can be viewed as a combination of a downsampled positive frequency projection filter with a traditional *dual-band* real wavelet transform and, therefore, at the finest decomposition level, the CWT subband has a resolution $4\times$ lower than the real input signal. Furthermore, the mapping-based solution has been significantly less amenable to geometric modeling than the redundant representations. To enable such geometric modeling, a basic requirement in image coding applications, Felix et al. [3] propose a linear-phase, semi-orthogonal, directional NCWT design using a novel *tri-band* filter bank. The NCWT solution based on tri-band filters permits a natural, direct NCWT implementation using complex wavelet filters and a real scaling filter. Furthermore, at the finest decomposition level, the resulting complex subband has resolution $3\times$ lower than the real input signal. Fig.3 shows the 1D implementation of the NCWT transform based on the tri-band filter banks.

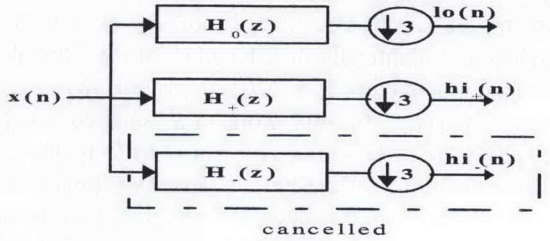

Figure 2: Filter bank of real NCWT [3].

Fig. 3 shows the 2D filter responses of the NCWT transform based on the tri-band filter bank. It is clearly indicated that the NCWT has an excellent directionality capability while keeping the transform non-expansive. Similar to its redundant counterparts, the NCWT transform can efficiently distinguish the opposite diagonal directions due to the use of two different filters to represent the diagonal features.

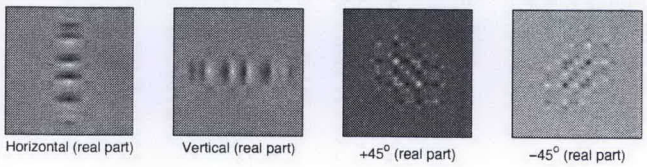

Figure 3: 2D Filter impulse responses for the NCWT (real parts only).

3 Information-Theoretic Data-Hiding Analysis

To derive the fundamental limits of watermarking and data hiding systems, we will follow the framework used in [1] where no a priori assumptions are made about the embedding and decoding functions. The recent theory developed in [1] establish the fundamental limits of the watermarking (and data hiding) problem.

3.1 Communications Model for Watermarking

In Moulin-Mihçak's framework [1], the watermarking system embeds or hides a watermark payload message M in a length-N host data sequence $S^N = (S_1, \cdots, S_N)$. Side-information $K^N = (K_1, \cdots, K_N)$, such as cryptographic key or host signal-dependant data, may used by the watermark embedding stage. The watermarked data is denoted by $X^N = (X_1, \cdots, X_N) = f_N(S^N, M, K^N)$. Watermark attackers, modeled by attack channels, intend to remove or at least make useless the embedded message M. The sequence $Y^N = (Y_1, \cdots, Y_N)$ represents the attacked watermarked sequence. To derive the data-hiding capacity, we assume that the host images can be "*correctly*" modeled as sequences of independent and identically distributed (i.i.d.) K-dimensional Gaussian random vectors $S \sim \mathcal{N}(0, R)$, where R is a $K \times K$ correlation matrix. In this work, the squared Euclidean distance, $d(x, y) = ||x - y||^2$, for $x, y \in \Re^K$ is used as the main distortion metric. Data-hiding capacity estimates for the scalar case, $K = 1$ (in this case $S \sim \mathcal{N}(0, \sigma^2)$ are presented in [1]. In this paper, we are mainly interested in the parallel representation of the outlined problem. Thus, the host data S is represented by means of K parallel Gaussian channels. In the latter case, the channel inputs are K independent sources $S_k, 1 \leq k \leq K$. Each channel S_k is modeled as a sequence of i.i.d. Gaussian random variables $\mathcal{N}(0, \sigma_k^2)$. Because the watermarking problem can be viewed as a game-theoretic problem between the data embedder and the attacker who is an intelligent opponent, game-theoretic analysis of the watermarking problem has been successfully formulated for both the scalar and vector cases [1]. In this game-theoretic framework [1], maximum distortion levels are specified for both the watermark embedder (D_1) and attacker (D_2). The maximum distortion imposed on the watermark embedder is given by [1]:

$$Ed^N(S^N, X^N) \leq D_1 \tag{1}$$

Attacks on embedded watermarks, modeled by specific channel models, are subject to distortion D_2 [1]:

$$Ed^N(S^N, Y^N) \leq D_2, \quad N \geq 1 \tag{2}$$

For a specific length-N data-hiding code, the data-hiding capacity $C(D_1, D_2)$ is defined as the supremum of all achievable rates R for distortions (D_1, D_2) [1].

Scalar Gaussian Channels: Under the distortion constraints Eqs. (1) and (2), the data-hiding capacity for scalar Gaussian channels is given by [1]:

$$C = \Gamma\left(\sigma^2, D_1, D_2\right) \triangleq \begin{cases} \frac{1}{2}\log\left(1 + \frac{D_1}{D}\right), & \text{if } D_1 < D_2 < \sigma^2 \\ 0, & \text{if } D_2 \geq \sigma^2 \end{cases} \tag{3}$$

where $D \triangleq \sigma^2 \frac{D_2 - D_1}{\sigma^2 - D_2}$. In practical watermarking applications where $\sigma^2 \gg D_1, D_2$, we have $D \sim D_2 - D_1$ and therefore:

$$C \sim \frac{1}{2} log\left(1 + \frac{D_1}{D_2 - D_1}\right) \tag{4}$$

Eq. (4) clearly indicates that the capacity is independent of the host signal variance σ^2.

Parallel Gaussian Channels: In this work, the parallel Gaussian case is of interest to us. The host signal, S^N, is decomposed into K channels using the NCWT transform. Each subsignal $S_k^{N_k}$, $1 \leq k \leq K$ consists of N_k samples. According to the model assumptions presented earlier, the subsignals $S_k^{N_k}$ are independent and are assumed to be Gaussian-distributed such as $\mathcal{N}(0, \sigma_k^2)$. Let d_{1k} and d_{2k} be the distortions introduced in channel k by the watermark embedder and attacker, respectively. Moulin and Mihçak [1] show that the allocation of powers $d_1 = \{d_{1k}\}$ and $d_2 = \{d_{2k}\}$ between channels, satisfies the overall distortion constraints:

$$\sum_{k=1}^{K} r_k d_{1k} \leq D_1 \text{ and } \sum_{k=1}^{K} r_k d_{2k} \leq D_2 \tag{5}$$

where r_k is the inverse subsampling factor in channel k given by: $r_k = \frac{N_k}{N}$. It is assumed that $\sum_{k=1}^{K} r_k = 1$. The rates given by Eq. (5) are subject to the following $3K$ constraints:

$$0 \leq d_{1k}, \quad d_{1k} \leq d_{2k}, \text{ and } d_{2k} \leq \sigma_k^2 \tag{6}$$

for $1 \leq k \leq K$. The data hiding capacity of parallel Gaussian channels is given by the following maximization-minimization relation, Eq. (7), subject to the $3K + 2$ constraints defined above [1]:

$$C = \max_{d_1} \min_{d_2} \sum_{k=1}^{K} r_k \Gamma\left(\sigma_k^2, d_{1k}, d_{2k}\right) \tag{7}$$

3.2 Models of Typical Images

Unlike in the case of redundant CWT transforms, the structure of the subbands emanating from NCWT decomposition have

similar structure, to some extent, to that obtained using real DWT decomposition (refer to Section 2 for details). This similarity in subband structure motivates us to investigate the suitability of well-established statistical models that were initially designed for real DWT wavelets. In these models [4], subbands' coefficients are modeled as Gaussian and generalized-Gaussian processes, respectively, with zero means and variances that depend on the coefficient location within each decomposition subband. In [4], it is assumed that the coefficients' variances belong to a finite set of values $\sigma_k^2, 1 \leq k \leq K$. In our work, we adopt the technique proposed in [1] to estimate representative values of $\sigma_k^2, 1 \leq k \leq K$. Fig. 4 shows the resulting 256 parallel channels in Lena image based on the real parts of the decomposition subbands.

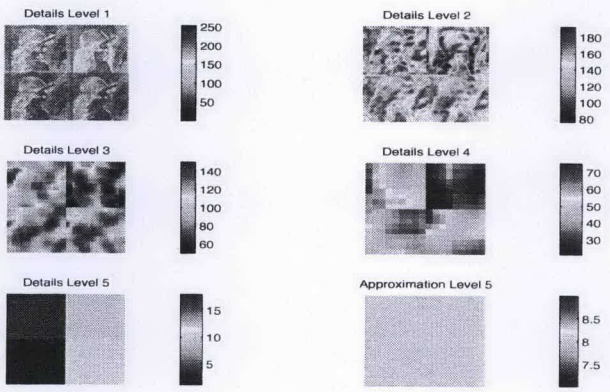

Figure 4: EQ-estimated 256 parallel Gaussian channels in Lena image (real parts of subbands only).

3.3 Estimates of Data-Hiding Capacities

In this section, we investigate the data-hiding capacity of typical natural test images. Analysis results are presented for four test images, Lena, Barbara, Baboon and Peppers. To derive the fundamental limits of watermarking and data hiding systems, we will follow the methodology used in [1] where no a priori assumptions are made about the embedding and decoding functions. Table 1 summarizes the capacity estimates for data-hiding. For comparison purposes, we also report the results for DWT (orthogonal Daubechies 8 and linear phase 9/7 filters) [1] and BMW [4] transforms. It is clear, from Table 1, that the NCWT transforms yield higher data-hiding capacity due to the inherent structure of the resulting decomposition. The ability to allow more embedding capacity is mainly attributed to the their ability to better characterize the texture content and the directional features of the source images.

4 Conclusions

In this paper, we have derived capacity estimates of data-hiding for NCWT transforms. Reported results clearly indicated that the latter transforms outperform the DWT and balanced multiwavelets in terms of data-hiding capacity. The substantial gain in capacity estimates is mainly due to the ability of NCWT transforms to explicitly characterize the phase information in the source images.

Image	D_1	$D_2 = 2D_1$		$D_2 = 5D_1$	
		NC	NC-Spike	NC	NC-Spike
Lena (D8)	10	27664	22080	3677	4818
Lena (9/7)		27233	21714	3651	4589
Lena (BMW)		31786	25820	4578	5642
Lena (NCWT)		**37512**	**30979**	**6061**	**6674**
Baboon (D8)	25	26347	26148	4018	5455
Baboon (9/7)		24212	25218	3781	5842
Baboon (BMW)		35041	33578	5468	6734
Baboon (NCWT)		**61394**	**57473**	**12555**	**11976**
Peppers (D8)	10	19422	20708	3042	4344
Peppers (9/7)		16922	17852	2790	3962
Peppers (BMW)		20030	19774	3170	4440
Peppers (NCWT)		**44004**	**33917**	**7127**	**6875**
Barbara (D8)	20	22840	24495	3683	5475
Barbara (9/7)		18289	20026	2868	4531
Barbara (BMW)		29910	31134	4969	6792
Barbara (NCWT)		**39045**	**37118**	**7041**	**8081**

Table 1: Total Data-Hiding Capacities (in bits) for images of size $N \times N = 512 \times 512$.

5 Acknowledgments

The author would like to thank Dr. Kivanç Mihçak, Dr. Felix Fernandes, Prof. Richard Baraniuk and Mr. Michael Wakin for providing valuable help during the preparation of this paper.

References

[1] P. Moulin and M. C. Mihçak, "A framework for evaluating the data-hiding capacity of image sources," *IEEE Trans. Image Processing*, vol. 11, no. 9, pp. 1029–1042, Sept. 2003.

[2] B. Chen and G. W. Wornell, "Quantization index modulation: A class of provably good methods for digital watermarking and information embedding," *IEEE Trans. Inform. Theory*, vol. 47, no. 5, pp. 1423–1443, May 2001.

[3] F. C. A. Fernandes, M. B. Wakin and R. G. Baraniuk, " Non-Redundant, Linear-Phase, Semi-Orthogonal, Directional Complex Wavelets," in *Proc. IEEE Int. Conf. Acoust., Speech, Signal Processing (ICASSP 2004)*, vol. 2, pp. 953–956, May 2004.

[4] L. Ghouti, A. Bouridane, M. K. Ibrahim, and S. Boussakta, "Digital image watermarking using balanced

multiwavelets," *IEEE Trans. on Signal Processing*, vol. 54, no. 4, pp. 1519–1536, Apr. 2006.